Excitable solitons in a semiconductor laser with a saturable absorber

Margherita Turconi,[1,*] Franco Prati,[2,3] Stéphane Barland,[1] and Giovanna Tissoni[1]

[1]*Université de Nice Sophia Antipolis, Institut Non Linéaire de Nice, CNRS UMR 7335, 1361 Route des Lucioles, F-06560 Valbonne, France*

[2]*Dipartimento di Scienza e Alta Tecnologia, Università dell'Insubria, Via Valleggio 11, I-22100 Como, Italy*

[3]*CNISM, Research Unit of Como, Via Valleggio 11, I-22100 Como, Italy*

(Received 6 August 2015; published 23 November 2015)

Self-pulsing cavity solitons may exist in a semiconductor laser with an intracavity saturable absorber. They show locally the passive Q-switching behavior that is typical of lasers with saturable absorbers in the plane-wave approximation. Here we show that excitable cavity solitons are also possible in a suitable parameter range and characterize their excitable dynamics and properties.

DOI: 10.1103/PhysRevA.92.053855 PACS number(s): 42.65.Tg, 42.65.Sf, 42.55.Px

I. INTRODUCTION

In recent years, optical dissipative solitons have been the object of extensive research in many different systems [1,2]. They are single-peaked optical localized structures, often called cavity solitons. Among the different optical systems where they may exist, semiconductor devices are particularly interesting in view of potential applications to telecommunications and optical information storing and processing [3,4].

A cavity soliton laser is an optical system which is able to emit cavity solitons in the absence of an injected coherent field. Different experimental realizations have been proposed where the amplifier is a semiconductor and the bistability mechanism can be induced either by a saturable absorber (both in intracavity [5,6] and in coupled-cavity configurations [7,8]) or by frequency selective feedback [9].

The semiconductor laser with an intracavity saturable absorber is the most interesting for applications, due to its compactness and the possibility of integration in an all-optical circuit. In such a system, cavity solitons were first predicted in Ref. [10], and the model was afterwards refined to include quadratic radiative recombination [11].

While most of the interest was initially concentrated in demonstrating the existence of stationary cavity solitons (CSs), more recently a drift instability leading to spontaneous soliton motion was predicted [12–14] and later an oscillatory instability affecting CSs was reported. These oscillating solitons and their interaction were studied in Ref. [15], where the existence of chaotic localized states was also numerically demonstrated.

On the other hand, excitability is a general dynamical behavior common to many different dynamical systems, consisting of a well-defined thresholdlike response upon perturbation, followed by a return to the initial (stable) state [16–19]. In optics, examples of excitable systems include optical amplifiers [20], lasers with optical feedback [21,22], lasers with saturable absorbers [23,24], lasers with optical injection [25], and active photonic crystals [26].

In the great majority of the existing literature, excitable optical systems have been analyzed in the plane-wave approximation, that is, in the absence of spatial effects. Noticeable exceptions are the studies on propagation of excitable pulses in the transverse space in a laser or absorber with optical injection [27,28] and a scheme which combines excitability and drifting localized states in a laser with a saturable absorber in the coupled-cavity configuration [29,30]. Another system that links excitability to localized structures is the Lugiato-Lefever model of a Kerr cavity, where excitability mediated by CSs has been demonstrated in Refs. [31,32].

Our aim here is to investigate the existence of excitable solitons in a semiconductor laser with an intracavity saturable absorber. As we show, such excitable solitons exist in a parametric region slightly below the laser threshold where, for some values of the parameters, the limit cycle in the phase space associated with the oscillating solitons becomes unstable and the only stable state is the laser-off solution. Under those conditions, a suitable localized address pulse is able to excite a transient solitonic pulse, provided its amplitude exceeds a certain excitability threshold. We stress that our system is excitable also in the plane-wave approximation [23,33], in contrast with Refs. [31,32].

In Sec. II we review the model describing a vertical cavity surface emitting laser (VCSEL) with a saturable absorber, and in Sec. II A we analyze the stability of stationary and oscillating CSs. In Secs. III and III A we study excitable CSs by analyzing the dependence of their peak intensity and of the delay time on the amplitude of the perturbation and by analyzing the dependence of the excitability threshold on the distance from the laser threshold. In Sec. III B we demonstrate that the shape of the excitable pulses is independent of the width of the perturbation so that, in addition to the usual temporal pulse reshaping, our excitable solitons also provide spatial reshaping. In Sec. III C we show that by tuning the injected field to the cavity soliton a large reduction of the excitability threshold can be achieved. Section IV is devoted to the conclusions.

II. MODEL AND SELF-PULSING CAVITY SOLITONS

The dynamical equations for a VCSEL with an integrated absorber stage are [10]

$$\dot{F} = [(1 - i\alpha)D + (1 - i\beta)d - 1]F + i\nabla_{\perp}^2 F, \tag{1}$$

$$\dot{D} = -b_1[D(1 + |F|^2) - \mu], \tag{2}$$

$$\dot{d} = -b_2[d(1 + s|F|^2) + \gamma]. \tag{3}$$

*Present address: Observatoire de la Côte d'Azur-Laboratoire ARTEMIS, Bvd. de l'Observatoire CS 34229, F-06304 Nice, France.

 ©2015 American Physical Society

The dimensionless variables F, D, and d are, respectively, the slowly varying envelope of the electric field, the carrier density of the amplifier medium, and the carrier density of the absorber medium. The transverse Laplacian operator $\nabla_\perp^2 = \partial_{xx}^2 + \partial_{yy}^2$ represents diffraction in the paraxial approximation. The parameters α and β are the linewidth enhancement factors of the semiconductor materials; μ and γ are the pump and absorption parameters for the active and passive material; b_1 and b_2 are the ratio of the photon lifetime to the carriers lifetimes in the two materials, and s is the saturation parameter. Time is scaled to the cavity lifetime and the transverse coordinates x and y are scaled to the diffraction length. This means that, for VCSELs, the time unit (t.u.) is of the order of 10 ps and the spatial unit (s.u.) is of the order of a few microns. We also define the parameter r as the ratio of the carrier lifetimes in the amplifier and in the absorber:

$$r = \frac{b_2}{b_1} = \frac{\tau_{\text{amp}}}{\tau_{\text{abs}}}. \tag{4}$$

The parameters r and and μ vary in our studies while the other parameters are kept fixed:

$$\gamma = 0.5, \quad s = 10, \quad \alpha = 2, \quad \beta = 0.2, \quad b_1 = 0.01. \tag{5}$$

All values are the same as those in Ref. [10] except β, which here is set more realistically different from zero. Notice, however, that for larger positive values of β the CSs are invariably unstable. The consolidated technique to excite CSs in the position (x_0, y_0) is to inject a suitable field for a short period, τ_{inj}. We use a field of the form

$$F_{\text{inj}} = |F_{\text{inj}}| e^{i\phi_{\text{inj}}} e^{-i\omega_{\text{inj}} t} e^{-\frac{(x-x_0)^2+(y-y_0)^2}{2\sigma_{\text{inj}}^2}}, \tag{6}$$

i.e., a field with Gaussian profile in space with amplitude $|F_{\text{inj}}|$, width σ_{inj}, phase ϕ_{inj}, and frequency ω_{inj}. In a laser with saturable absorber, however, the phase is irrelevant, since the laser is in the off state before injection. The other injection parameters are chosen as in [10]

$$\omega_{\text{inj}} = 0, \quad \sigma_{\text{inj}} = 3, \quad |F_{\text{inj}}| = 1.5, \quad \tau_{\text{inj}} = 100. \tag{7}$$

The frequency $\omega_{\text{inj}} = 0$ corresponds to the cavity resonance. The peak intensity and the frequency of the stationary CSs obtained for $r = 0.45$ are plotted in Fig. 1 as functions of the active material pump parameter μ. The zero and nonzero homogenous plane-wave solutions (modulationally unstable for this set of parameters) are also shown for comparison. We were able to switch-on CSs in the interval $1.415 \leqslant \mu \leqslant 1.49$ where they coexist with the stable homogenous nonlasing solution.

The stability analysis of CSs in the plane of the parameters (μ, r) reveals a scenario similar to that reported in Ref. [12] for a slightly different model which includes the effects of carrier radiative recombination [11,34]. The stability domain of CSs is shown in the Fig. 2(a). With respect to Ref. [12], the stability domain is shifted towards smaller values of r. As a consequence, no stable CS exists when the recombination times of the two materials are very close to one another ($r \approx 1$).

For a given μ, the stationary CSs are stable in a range of r which lies inside the stability domain of the lasing homogeneous solution with respect to a Hopf instability, whose boundary is given approximately by the condition

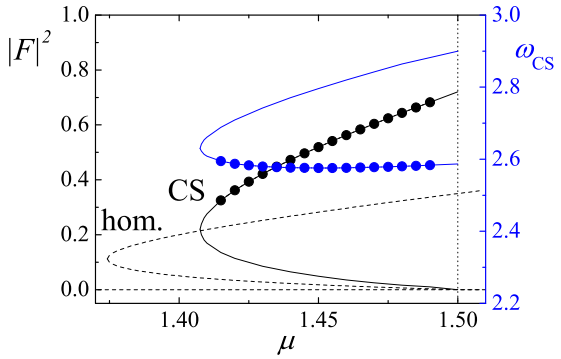

FIG. 1. (Color online) Homogenous stationary solution (dashed line), peak intensity (black lower solid line), and frequency of stationary CSs (blue upper solid line) as functions of μ. The symbols indicate the stable CSs. The system parameters are those in Eq. (5) with $r = 0.45$. The CSs are switched-on by the injected field in Eq. (6) with injection parameters as in Eq. (7). The laser threshold is $\mu = 1.5$.

$\mu < r^2\gamma s$ or $r > \sqrt{\mu/\gamma s}$ [10,35]. Below the lower limit of the CS stability domain (Fig. 2(a), red line and symbols) a drift instability associated with real eigenvalues gives rise to spontaneously moving solitons [12]. Above the upper limit there is a region where oscillating CSs are stable [15], which is shown enlarged in Fig. 2(b).

A. Self-pulsing cavity solitons

We characterize the CS oscillations by measuring the period and the maximum and minimum values of the peak oscillations as a function of μ. The values measured for $r = 0.5$ are shown in Fig. 3. Both the amplitude of the peak oscillations and the period increase with decreasing μ.

The same study can be done by fixing the value of μ (for example, $\mu = 1.45$) and by letting the parameter r vary. Here, on the contrary, both the amplitude of the peak oscillations and the period increase with r ([36]).

As shown in Fig. 3, for $\mu = 1.465$ the CS is stationary so the intensity is constant. For smaller μ (about $\mu = 1.4635$) the stationary CS undergoes a Hopf bifurcation. The amplitude of the oscillations increases rapidly as μ decreases and very soon a regime of nonlinear pulses similar to Q switching is reached: the intensity is close to zero for most of the time except for short periodic intervals [see inset of Fig. 3(a)]. The maximum pulse intensity is about seven times the intensity of a stationary CS for $\mu = 1.45$ and it grows as μ decreases.

The period is around 125 t.u. at the onset of the oscillations (roughly 1.25 ns) and it increases rapidly over 270 t.u. (roughly 2.7 ns), showing a clear divergence as μ approaches the left boundary for the existence of self-pulsing CS (the last point in Fig. 3 is $\mu = 1.4472$). In particular, as shown by the red dashed line in Fig. 3(b), the period of the oscillating CS diverges as the logarithm of the distance from the bifurcation, indicating that the oscillations disappear through a saddle-loop or homoclinic bifurcation.

For smaller values of μ, the period of the oscillations initially increases, then the pulsing CS destabilizes and after some tens of oscillations (in the proximity of the critical value)

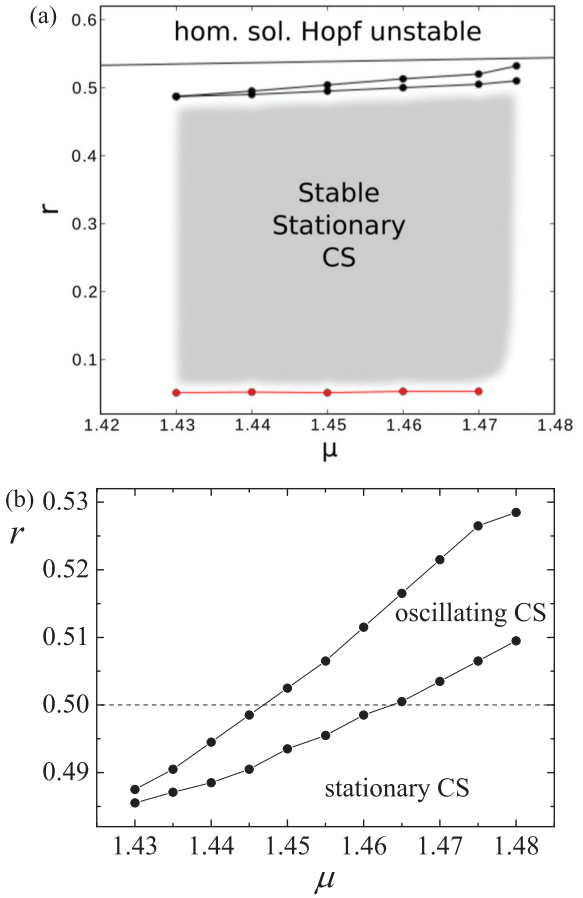

FIG. 2. (Color online) (a) Stability domain of the stationary CSs (gray region), in the plane of parameters r and μ. The black continuous line limits the region where the homogeneous solution is Hopf unstable. In the region between the black (upper) solid lines with symbols self-pulsing CSs are stable. In correspondence with the red (lower) line with symbols the CSs undergo a drift instability. (b) Zoom of the upper part of the diagram showing the stability domain of the self-pulsing CSs. Below the displayed lower boundary, CSs are stationary; beyond the upper boundary, they decay either to the nonlasing state (smaller μ) or to a complex spatiotemporal state (larger μ). The horizontal dashed line corresponds to the value $r = 0.5$, used in Fig. 3.

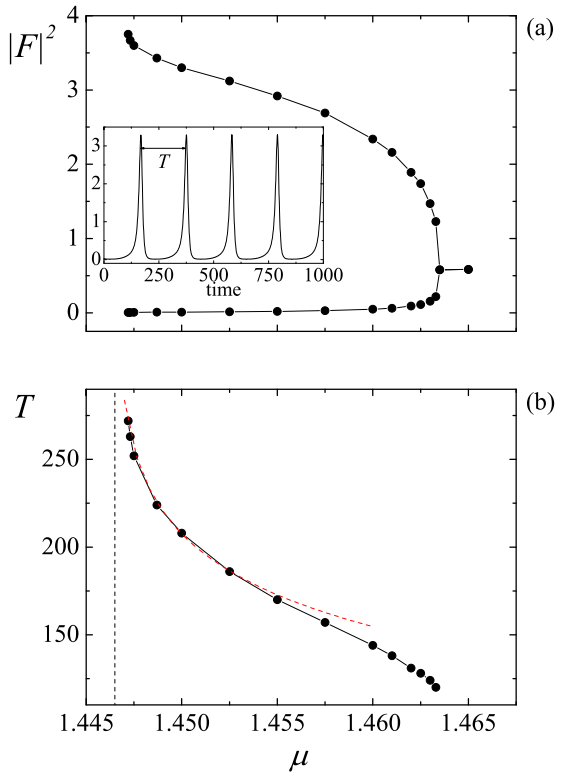

FIG. 3. (Color online) (a) Maximum and minimum values of the peak intensity of an oscillating CS as a function of μ for $r = 0.5$. The inset is the time trace for $\mu = 1.45$. (b) Corresponding period of the intensity oscillations. The dashed red line is a fit of the six leftmost points with the function $T = T_0|\ln[(\mu - \mu_{\rm hom})/a]|$. The calculated values of the fitting parameters are $T_0 = 39.134$, $\mu_{\rm hom} = 1.4465$, and $a = 0.70323$. The dashed vertical line indicates the position of the homoclinic bifurcation $\mu = \mu_{\rm hom}$. Other parameters are as in Eq. (5).

it switches-off spontaneously. Such a bifurcation from a stable limit cycle (self-pulsing CS) to a fixed point (homogeneous nonlasing state) makes our system a candidate for exhibiting excitability.

III. EXCITABLE CAVITY SOLITONS

Excitability is a feature of a nonlinear dynamical system defined by the response to an external perturbation. Perturbations smaller than a given threshold are exponentially damped and the system remains in its stable state. If the perturbation exceeds that threshold the system performs a large excursion in the phase space before coming back to its initial stable state.

For the fixed pump value $\mu = 1.47$ we apply a perturbation to the zero-intensity homogeneous solution and compare the response of the system for three different values of r. One value ($r = 0.48$) lies within the stability domain of stationary CSs, another one ($r = 0.51$) lies within the stability domain of self-pulsing CSs, and the third one ($r = 0.56$) lies outside both stability domains. We use the same perturbation as in Eq. (6), with $|F_{\rm inj}| = 1.25$, $\tau_{\rm inj} = 50$, and $\sigma_{\rm inj} = 3$.

In Fig. 4(a) the time evolution of the intensity in the central point of the applied perturbation is displayed. Three different behaviors are observed, depending on the value of r: (i) for $r = 0.48$ (red line), the system reaches, through damped oscillations, the stationary CS solution (the process takes about 5000 t.u.); (ii) for $r = 0.51$ (blue line), the system approaches the self-pulsing CS solution through growing oscillations; and (iii) for $r = 0.56$ (black line), the system emits a short pulse and goes back to the zero-intensity solution.

In Fig. 4(b) we show the corresponding trajectories in the sub-phase-space $(D + d - 1,\ |F|^2)$. The combination $D + d - 1$ represents the net gain (difference of gain and nonlinear and linear losses). In cases (i) and (ii) the system has two stable attractors: the nonlasing state (A) and the stationary CS (C) in case (i), and the nonlasing state (A) and the limit cycle corresponding to the self-pulsing CS solution in case (ii). The system can go from one attractor to the other provided the applied perturbation makes it go over the saddle point, *approximately given by* the unstable CS (B). In case (iii), instead, only the nonlasing state is stable and the trajectory (black line) presents the typical behavior of

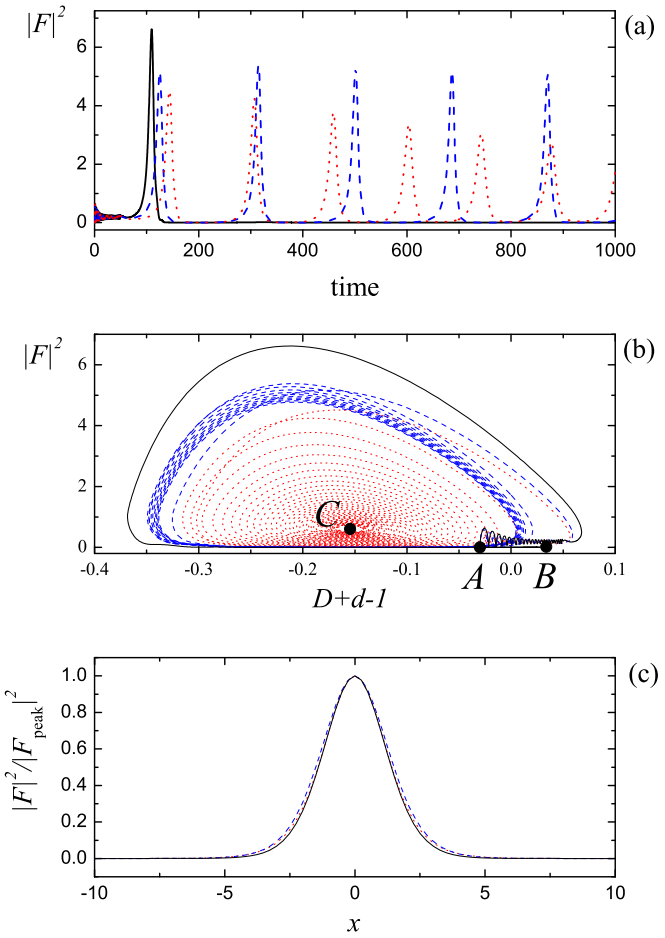

FIG. 4. (Color online) Response of the system to a local Gaussian perturbation for three different values of r: 0.48 (red dotted lines), 0.51 (blue dashed lines), and 0.56 (black solid lines), and $\mu = 1.47$. The perturbation parameters are $|F_{\rm inj}| = 1.25$, $\tau_{\rm inj} = 50$, and $\sigma_{\rm inj} = 3$. (a) Time evolution of the intensity in the central point of the applied perturbation. (b) Corresponding trajectories in a phase-space section: intensity $|F|^2$ vs net gain $(D + d - 1)$. A is the nonlasing state, B is the unstable CS belonging to the negative slope branch, and C is the CS solution belonging to the positive slope branch, which is stable for $r = 0.48$ and unstable for both $r = 0.51$ (oscillating CS stable) and $r = 0.56$ (oscillating CS unstable). (c) Spatial profiles of the stationary ($r = 0.48$), self-pulsing ($r = 0.51$), and excitable ($r = 0.56$) CSs. The curves are normalized to their maximum value. No matter what is the temporal behavior, light emission is localized in the same spatial profile.

excitability. The system, once it has overtaken the saddle, performs a large trajectory around the limit cycle which is no longer stable and it finally comes back to the stable nonlasing state. Finally, Fig. 4(c) shows that the normalized spatial profiles of the stationary, oscillating, and excitable CSs (the last two measured in correspondence with the maximum intensity) are almost undistinguishable.

A. Excitability threshold and delay

In order to characterize the excitable behavior of case (iii) we investigate the dependence on the injected pulse amplitude of the peak pulse intensity and of the time delay, measured

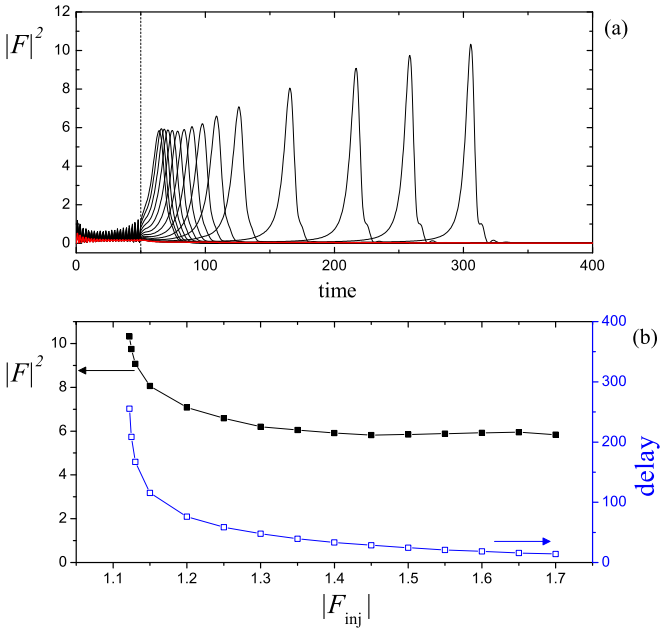

FIG. 5. (Color online) (a) Time evolution of the peak intensity in response to perturbations with different amplitudes. For a weak perturbation ($|F_{\rm inj}| = 1.122$) the system relaxes into the nonlasing state (red or light gray line); for larger perturbations a pulse is emitted before coming back to the nonlasing state. The intensity oscillations during injection (before the dashed vertical line) are due to the beating between the perturbation frequency and the CS frequency. The laser parameters are $\mu = 1.47$ and $r = 0.56$. The perturbation parameters are $\tau_{\rm inj} = 50$ (dashed vertical line) and $\sigma_{\rm inj} = 3$. (b) Intensity of the pulse emitted by the system as a function of the amplitude of the injected beam $|F_{\rm inj}|$ and corresponding delay time of the emitted pulse measured from the end of the injected pulse.

from the end of the applied perturbation. In Fig. 5(a) the red line shows the response to a perturbation with insufficient amplitude ($|F_{\rm inj}| = 1.122$), which causes just a small hump in the intensity before it relaxes to zero, while the black lines are the excitable pulses observed with amplitudes from 1.25 to 1.7. The peak intensity of the emitted pulse and the delay between pulse injection and pulse emission as functions of the perturbation amplitude $|F_{\rm inj}|$ are depicted in Fig. 5(b). Typically, excitability is characterized by a pulse height almost independent of the perturbation amplitude and a delay diverging at threshold and monotonically decreasing as the perturbation amplitude is increased. While the latter feature is present in Fig. 5(b), we observe that the peak intensity of the pulse increases approaching the excitability threshold and remains almost constant for larger perturbations.

We interpret this phenomenon as a consequence of the fact that the triggering pulse is not perfectly matched neither in spatial shape nor in frequency with the excitable pulse. Close to threshold this double mismatch is in part dynamically compensated by the system during the relatively long buildup stage of the pulse, and the emitted intensity can reach the largest values. Conversely, well above the excitability threshold the response of the system is very fast, so that

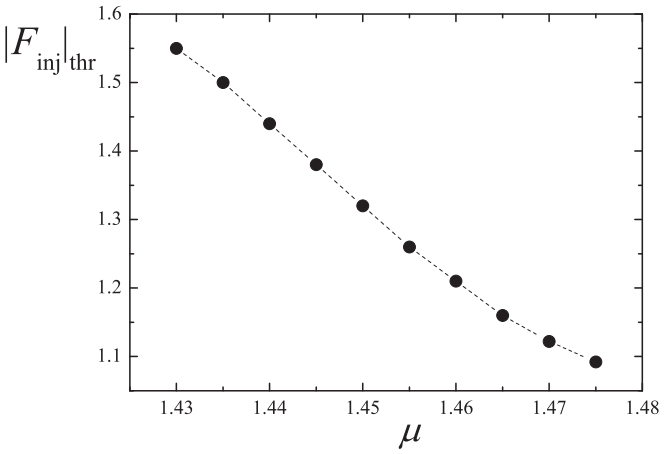

FIG. 6. The excitability threshold as a function of the pump parameter μ for $r = 0.56$ and injection at the cavity frequency $\omega = 0$. The injection parameters are $\tau_{inj} = 50$ and $\sigma_{inj} = 3$.

the effects of the mismatch are not compensated for and the emitted intensity is consequently reduced.

The excitable behavior is found for all the considered values of the pump parameter: $1.43 \leqslant \mu \leqslant 1.475$ at $r = 0.56$. The excitability threshold decreases as the current is increased as shown in Fig. 6. This can be understood from the fact that for higher pumping of the amplifier, the unstable CSs get closer to the nonlasing solution (they collide at the laser threshold).

The interesting aspect is that the excitable behavior is confined in a region of the transverse plane that matches the stationary CS profile. Therefore we claim that we are observing excitable CSs (or excitable localized structures) to distinguish our case from the plane-wave excitable behavior reported in lasers with a saturable absorber [23,33].

Localized excitable structures have been investigated in Kerr cavities [31,32,37]. With respect to those works we stress that we use a different, and more realistic, procedure to excite the pulses, consisting of a perturbation of a stable state (the nonlasing state) instead of a perturbation of an unstable state (the localized structure in the unstable negative slope branch).

B. Temporal and spatial beam reshaping

One useful application of excitability in optics consists of the fact that the temporal profile of the excited pulse is independent of that of the applied perturbation. Therefore, for instance, Gaussian, rectangular, and δ-like perturbations all yield pulses with the same shape [33].

Our localized excitable structures have the additional property of reshaping the *spatial* profile of the perturbation. We demonstrate this by injecting three Gaussian-shaped pulses with different widths, $\sigma_{inj} = 2$, 3, and 4, and the same rectangular profile of duration $\tau_{inj} = 50$. The amplitude $|F_{inj}|$ is chosen close to the excitability threshold in order to have a similar temporal response in all cases. It is reasonable to assume that the excitability threshold is related to the injected energy,; i.e., it is proportional to the quantity $|F_{inj}|^2\sigma_{inj}^2\tau_{inj}$. Since in these simulations $\tau_{inj} = 50$ is kept constant, the threshold amplitude should be inversely proportional to the beam width σ_{inj}. Actually, this proportionality law is a good

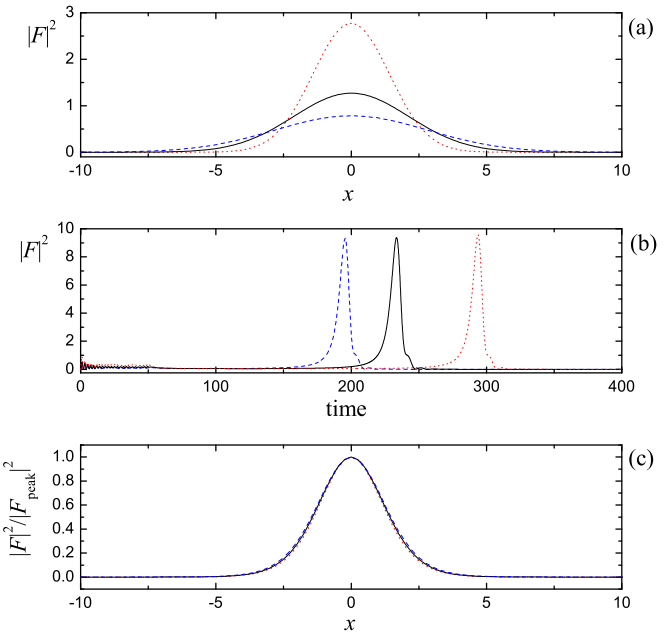

FIG. 7. (Color online) Three different injected pulses and the resulting responses. (a) Spatial intensity profiles of the injected Gaussian pulses. (b) Time evolution of the peak intensity from the beginning of the injection. (c) Normalized spatial intensity profile corresponding to the peak of the excitable response. The injection parameters are $\sigma_{inj} = 2$ and $|F_{inj}| = 1.666$ (red dotted lines); $\sigma_{inj} = 3$ and $|F_{inj}| = 1.13$ (black solid lines); and $\sigma_{inj} = 4$ and $|F_{inj}| = 0.89$ (blue dashed lines). For all of them $\tau_{inj} = 50$ and $\omega_{inj} = 0$.

approximation of reality. In our simulations the amplitude $|F_{inj}|$ is such that $|F_{inj}|\sigma_{inj} = 3.33$, 3.39, and 3.56 for $\sigma_{inj} = 2$, 3, and 4, respectively. The spatial intensity profile of the three perturbations is shown in Fig. 7(a).

The temporal and spatial profiles of the excited pulses are illustrated for comparison in Figs. 7(b)and 7(c). The three temporal profiles shown in 7(b) are very similar, although the delay times are slightly different. They can be approximated by a Gaussian of temporal HWHM $\approx$13 and a height between 9.34 and 9.58. The three scaled spatial profiles taken at the pulse maximum are shown superimposed in Fig. 7(c). They are undistinguishable and well approximated by a Gaussian with a spatial HWHM $\approx$1.35, i.e., narrower than all three perturbations.

C. Low threshold excitability in response to a perturbation frequency matched with the CS

The injection frequency is a key parameter in nucleation processes, and experimentally a frequency matched perturbation is much more efficient [38]. It was shown in Ref. [39] that, in the case of a stationary CS, injection of a writing beam at the soliton frequency ω_{CS} allows one to reduce the energy threshold with respect to injection at the cavity frequency ($\omega_{inj} = 0$). We show that this result also applies to the excitability threshold.

The frequency of the CS for $\mu = 1.47$ is $\omega_{CS} = 2.578$ (see Fig. 1). By injecting a perturbation oscillating at that frequency we were able to reduce both the injection time and

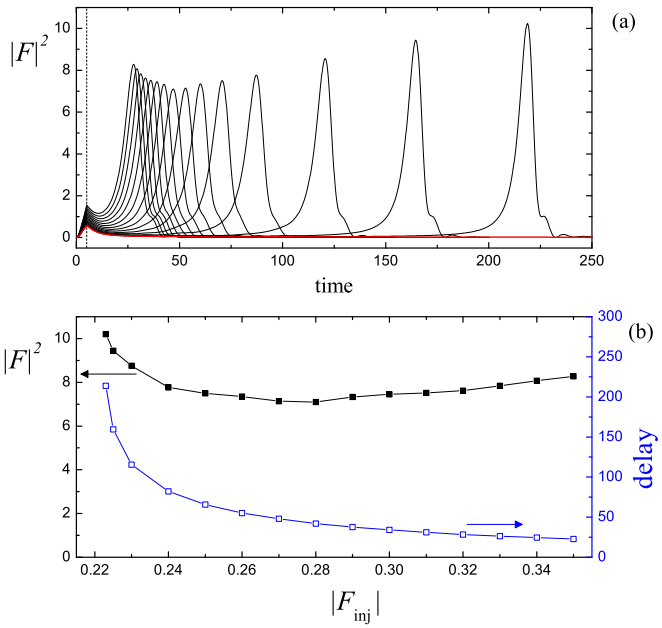

FIG. 8. (Color online) Excitable response for $\omega_{inj} = \omega_{CS}$. Panels (a) and (b) are the same as in Fig. 5. The other injection parameters are $\sigma_{inj} = 3$ and $\tau_{inj} = 5$.

the amplitude of the perturbation by an order of magnitude, resulting in an injected energy which is 3 orders of magnitude smaller.

Figure 8 must be compared with Fig. 5 obtained with $\omega_{inj} = 0$. The width of the injected field is $\sigma_{inj} = 3$ in both figures but in Fig. 8 the injection time is $t_{inj} = 5$ instead of 50 and, nonetheless, the excitability threshold is found at a smaller value of the injected amplitude $|F_{inj}| = 0.223$ instead of 1.122.

On the other hand the dependence of the peak intensity and of the delay time, as reported in Figs. 5(b) and 8(b), is very similar. Here the increase in the emitted pulse intensity close to the excitability threshold is less pronounced than that in Fig. 5, which corroborates our previous interpretation of this phenomenon because now the frequency mismatch is removed (see Sec. III A).

In Fig. 9 we show how the excitability threshold increases as we move away from the laser threshold $\mu = 1.5$. This figure must be compared with the analogous Fig. 6 obtained with a perturbation oscillating at the cavity frequency $\omega = 0$. Injection at the CS frequency results in a linear dependence of the threshold on the pump μ and, as observed before for $\mu = 1.47$, in a substantial reduction of the switching energy.

We were not able to calculate numerically the excitability threshold in the vicinity of the laser threshold because, as shown in Fig. 1, no stable CS exists in that interval. Notice, however, that a linear interpolation of the data shows that the excitability threshold could not vanish at the laser threshold $\mu = 1.5$ (the interpolated value is $|F_{inj}|_{thr} \approx 0.13$). This represents a marked difference with respect to the plane-wave model [33]. It implies that the excitation of a localized pulse from noise in a spatially extended system is much less likely than in a pure temporal one.

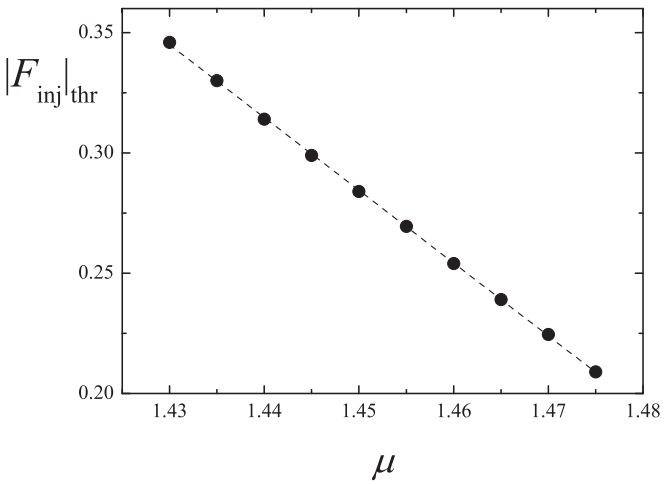

FIG. 9. The excitability threshold as function of the pump parameter μ for $r = 0.56$ and injection at the CS frequency ω_{CS}. The injection parameters are $\tau_{inj} = 5$ and $\sigma_{inj} = 3$.

IV. CONCLUSIONS

We have studied numerically the stability of CSs in a VCSEL with a saturable absorber using the ratio of the carrier lifetimes in the passive and in the active material (r) and the pump parameter in the active region (μ) as control parameters. In a certain parameter region, stationary CSs develop a Q-switching instability, and self-pulsing CSs are found to be stable and to coexist with the homogeneous nonlasing solution.

Beyond the bifurcation from the self-pulsing CS regime to the nonlasing solution, we have demonstrated the existence of excitable laser CSs. They appear as a short laser pulse localized in space, arising from the stable nonlasing state in response to a local perturbation that exceeds a characteristic threshold. After the emission of the pulse, the system comes back to the initial nonlasing stable state. The spatial profile of the emitted pulse matches the profile of stable stationary or self-pulsing CSs found in the same system.

We refrain from characterizing this excitable behavior with a numeric label, since it is known that at least 72 different possibilities exist [18]. According to the classification of Ref. [18] we are in the "subHopf/homoclinic" case, because the quiescent state loses stability through a subcritical Andronov-Hopf bifurcation and the oscillating regime through a homoclinic bifurcation.

Notice, however, that in our case the oscillating state is *local*, whereas the quiescent state is *global*. Therefore in our system pulses can be excited in any position of the transverse plane, and several pulses can be excited simultaneously.

We have shown that excitable laser CSs can also be used for pulse reshaping by proving that the shape of the output pulse does not depend on the shape of the input pulse. The output pulse does not depend on the input frequency either. We were able to trigger an excitable localized structure with input pulses at the cavity frequency and at the CS frequency. Injection at the CS frequency allows one to reduce the energy of the trigger

pulse by a factor 1000 with respect to the injection at the cavity frequency.

We note that in experiments on distant coupled absorber-amplifier systems no excitability has been observed in the absence of drift, contrary to the present results [38]. We believe this can be explained by very slow time scale of the field variable in the coupled system.

Excitable CSs may represent a new tool in all-optical processing of information [40]. They have been already predicted in an optical cavity filled with a Kerr medium [31]. There, excitability is said to be mediated by localized structures, because it is strictly related to the presence of the spatial degrees of freedom and it disappears in the plane wave (PW) case. Here on the contrary, we are dealing with a system that is known to be excitable even in the PW limit [33]. We believe that the results presented here could also serve in the interpretation of experiments in coupled arrays of micropillar lasers with saturable absorbers.

ACKNOWLEDGMENTS

We acknowledge support from the Agence Nationale de la Recherche ANR-Jeunes Chercheurs Project MOLOSSE (Grant No. ANR-12-JS04-0002-01, www.molosse.org).

[1] R. Kuszelewicz, S. Barbay, G. Tissoni, and G. Almuneau, Eur. Phys. J. D **59**, 1 (2010).
[2] T. Ackemann, W. J. Firth, and G. L. Oppo, in *Advances in Atomic Molecular and Optical Physics*, edited by E. Arimondo, P. R. Berman, and C. C. Lin (Academic Press, San Diego, 2009), Vol. 57, pp. 323–421.
[3] S. Barland, J. R. Tredicce, M. Brambilla, L. A. Lugiato, S. Balle, M. Giudici, T. Maggipinto, L. Spinelli, G. Tissoni, T. Knoedl *et al.*, Nature (London) **419**, 699 (2002).
[4] L. Lugiato, F. Prati, and M. Brambilla, *Nonlinear Optical Systems* (Cambridge University Press, Cambridge, UK, 2015).
[5] T. Elsass, K. Gauthron, G. Beaudoin, I. Sagnes, R. Kuszelewicz, and S. Barbay, Appl. Phys. B **98**, 327 (2010).
[6] T. Elsass, K. Gauthron, G. Beaudoin, I. Sagnes, R. Kuszelewicz, and S. Barbay, Eur. Phys. J. D **59**, 91 (2010).
[7] P. Genevet, S. Barland, M. Giudici, and J. R. Tredicce, Phys. Rev. Lett. **101**, 123905 (2008).
[8] P. Genevet, S. Barland, M. Giudici, and J. R. Tredicce, Phys. Rev. A **79**, 033819 (2009).
[9] Y. Tanguy, T. Ackemann, W. J. Firth, and R. Jäger, Phys. Rev. Lett. **100**, 013907 (2008).
[10] M. Bache, F. Prati, G. Tissoni, R. Kheradmand, L. Lugiato, I. Protsenko, and M. Brambilla, Appl. Phys. B **81**, 913 (2005).
[11] F. Prati, P. Caccia, G. Tissoni, L. Lugiato, K. Mahmoud Aghdami, and H. Tajalli, Appl. Phys. B **88**, 405 (2007).
[12] F. Prati, G. Tissoni, L. A. Lugiato, K. M. Aghdami, and M. Brambilla, Eur. Phys. J. D **59**, 73 (2010).
[13] H. Vahed, R. Kheradmand, H. Tajalli, G. Tissoni, L. A. Lugiato, and F. Prati, Phys. Rev. A **84**, 063814 (2011).
[14] G. Tissoni, K. M. Aghdami, M. Brambilla, and F. Prati, Eur. Phys. J.: Spec. Top. **203**, 193 (2012).
[15] H. Vahed, F. Prati, M. Turconi, S. Barland, and G. Tissoni, Philos. Trans. R. Soc., A **372**, 20140016 (2014).
[16] A. Hodgkin, J. Physiol. **107**, 165 (1948).
[17] A. Hodgkin, A. Huxley, and B. Katz, J. Physiol. **116**, 341 (1952).
[18] E. M. Izhikevich, Int. J. Bifurcation Chaos **10**, 1171 (2000).
[19] M. Izhikevich, *Dynamical Systems in Neuroscience: The Geometry of Excitability and Bursting* (MIT Press, Cambridge, MA, 2007).
[20] S. Barland, O. Piro, M. Giudici, J. R. Tredicce, and S. Balle, Phys. Rev. E **68**, 036209 (2003).
[21] M. Giudici, C. Green, G. Giacomelli, U. Nespolo, and J. R. Tredicce, Phys. Rev. E **55**, 6414 (1997).
[22] M. Turconi, B. Garbin, M. Feyereisen, M. Giudici, and S. Barland, Phys. Rev. E **88**, 022923 (2013).
[23] F. Plaza, M. G. Velarde, F. T. Arecchi, S. Boccaletti, M. Ciofini, and R. Meucci, Eur. Phys. Lett. **38**, 85 (1997).
[24] S. Barbay, R. Kuszelewicz, and A. M. Yacomotti, Opt. Lett. **36**, 4476 (2011).
[25] D. Goulding, S. P. Hegarty, O. Rasskazov, S. Melnik, M. Hartnett, G. Greene, J. G. McInerney, D. Rachinskii, and G. Huyet, Phys. Rev. Lett. **98**, 153903 (2007).
[26] M. Brunstein, A. M. Yacomotti, I. Sagnes, F. Raineri, L. Bigot, and A. Levenson, Phys. Rev. A **85**, 031803 (2012).
[27] P. Coullet, D. Daboussy, and J. R. Tredicce, Phys. Rev. E **58**, 5347 (1998).
[28] F. Marino and S. Balle, Phys. Rev. Lett. **94**, 094101 (2005).
[29] M. Turconi, M. Giudici, and S. Barland, Phys. Rev. Lett. **111**, 233901 (2013).
[30] P. Parra-Rivas, D. Gomila, M. A. Matías, and P. Colet, Phys. Rev. Lett. **110**, 064103 (2013).
[31] D. Gomila, M. A. Matías, and P. Colet, Phys. Rev. Lett. **94**, 063905 (2005).
[32] D. Gomila, A. Jacobo, M. A. Matías, and P. Colet, Phys. Rev. E **75**, 026217 (2007).
[33] J. L. A. Dubbeldam, B. Krauskopf, and D. Lenstra, Phys. Rev. E **60**, 6580 (1999).
[34] H. Vahed, F. Prati, H. Tajalli, G. Tissoni, and L. Lugiato, Eur. Phys. J. D **66**, 148 (2012).
[35] T. Erneux, J. Opt. Soc. Am. B **5**, 1063 (1988).
[36] M. Turconi, Ph.D. thesis, Ecole Doctorale de Sciences Fondamentales et Appliquées, Université de Nice–Sophia Antipolis, 2013.
[37] A. Jacobo, D. Gomila, M. A. Matías, and P. Colet, Phys. Rev. A **78**, 053821 (2008).
[38] M. Turconi, M. Giudici, and S. Barland, Philos. Trans. R. Soc., A **372**, 20140004 (2014).
[39] K. M. Aghdami, F. Prati, P. Caccia, G. Tissoni, L. A. Lugiato, R. Kheradmand, and H. Tajalli, Eur. Phys. J. D **47**, 447 (2008).
[40] A. Jacobo, D. Gomila, P. Colet, and M. Matias, Photonics Society Winter Topical Meeting Series (WTM) **10**, 122 (2010).